

Trapping of volatile fission products by C60

Kuganathan, N., Arya, A. K., Rushton, M. J. D. & Grimes, R. W.

Published PDF deposited in Coventry University's Repository

Original citation:

Kuganathan, N, Arya, AK, Rushton, MJD & Grimes, RW 2018, 'Trapping of volatile fission products by C60' Carbon, vol. 132, pp. 477-485.

<https://dx.doi.org/10.1016/j.carbon.2018.02.098>

DOI 10.1016/j.carbon.2018.02.098

ISSN 0008-6223

Publisher: Elsevier

© 2018 The Authors. Published by Elsevier Ltd. This is an open access article under the CC BY license

(<http://creativecommons.org/licenses/by/4.0/>).

Copyright © and Moral Rights are retained by the author(s) and/ or other copyright owners. A copy can be downloaded for personal non-commercial research or study, without prior permission or charge. This item cannot be reproduced or quoted extensively from without first obtaining permission in writing from the copyright holder(s). The content must not be changed in any way or sold commercially in any format or medium without the formal permission of the copyright holders.



Trapping of volatile fission products by C₆₀

Navaratnarajah Kuganathan^{a,*}, Ashok K. Arya^b, Michael J.D. Rushton^{a,c},
Robin W. Grimes^a

^a Department of Materials, Imperial College London, London, SW7 2AZ, UK

^b Material Science Division, Bhabha Atomic Research Centre, Trombay, Mumbai, 400 085, India

^c College of Physical and Applied Sciences, Bangor University, Bangor, Gwynedd, LL57, UK

ARTICLE INFO

Article history:

Available online 27 February 2018

Keywords:

C₆₀
DFT
Fission products
Encapsulation energy
Filters

ABSTRACT

Carbon based filters provide important safety barriers that remove volatile fission products from gas streams. The capacity and efficiency of a filter to trap fission products depends upon the strength of the interaction between the fission products and the filter material. In this study, we apply density functional theory together with a dispersion correction (DFT + D) to predict structures and energies of volatile fission product atoms and molecules trapped by buckminsterfullerene (C₆₀). Endohedral encapsulation energies and exohedral association energies show that Rb and Cs are strongly trapped as ions, each transferring approximately one electron to C₆₀. Kr and Xe are weakly trapped atoms with Xe showing a preference for exohedral association and Kr for endohedral encapsulation. Br, I and Te, while strongly trapped from atoms (and assuming charge from C₆₀) are thermodynamically more stable as neutral covalently bonded Br₂, I₂ and Te₂ molecules weakly trapped through van der Waals forces, exohedrally. Heteronuclear CsBr and CsI were also considered. Both molecules were non-bonded to C₆₀ with similar association energies to those exhibited by Br₂, I₂ and Te₂.

© 2018 The Authors. Published by Elsevier Ltd. This is an open access article under the CC BY license (<http://creativecommons.org/licenses/by/4.0/>).

1. Introduction

Gaseous effluents, generated during processing of spent fuel, contain radioactive volatile species including alkali metals, halogens and noble gases [1]. Among these, species such as iodine and strontium can be concentrated by the body, increasing the radiotoxic impact [2]. To minimize the hazard, radioactive species should be removed through either physical or chemical capture before the effluent is discharged to the atmosphere. Filters, in particular activated carbon filters, are mostly used to remove gaseous iodine species [3]. However, other porous materials including zeolites, silica, alumina and metal organic frameworks have been studied experimentally to improve the effectiveness of filters [3,4]. The search for alternative filter media that can trap volatile gases continues. Such materials must be thermodynamically stable, chemically active, have adequate mechanical properties and a high surface area, whilst still being manufacturable at scale in a cost-effective manner.

The buckyball structured carbon fullerenes and fullerites are

candidate materials for trapping volatile fission products (FP). They provide both inner and outer surface structures, high resistance to external chemical attack, are light weight and exhibit mechanical stability at high pressure and temperatures [5]. Buckminsterfullerene (C₆₀), consists of 60 carbon atoms and has been widely studied [6]. The interior and exterior of a C₆₀ molecule are surrounded by an electron charge density of conjugate π bonds each formed between two adjacent carbon atoms. The charge density of the inner space is therefore higher than the outer surface. The encapsulation of species within C₆₀ has been described in various experimental and theoretical studies: alkali metals (e.g. Li, K) [7,8], alkali earth metals (e.g. Ca, Sr and Ba) [7,8], radioactive isotopes (e.g. ¹⁵⁹Gd, ¹⁶¹Tb) [9,10], actinide metals (e.g. Lr) [11], non-metals (e.g. N, P) [12,13], noble gases (e.g. Ne, Ar) [14,15], transition metals (e.g. Tc, Fe) [16,17] and rare earth metals (e.g. La) [18]. These have all been considered either in the form of atoms or clusters. The external surface of C₆₀ has been studied theoretically for its interaction with transition metal atoms and clusters, and shown to provide a good catalyst for the activation of di-nitrogen molecules [19] and the storage of hydrogen [20]. Furthermore, the theoretical study by Ozdamar et al. [21] demonstrated the stability and electronic properties of Pt and Pd in the form of atoms and dimers interacting with the outer surface of C₆₀. Likewise, hydrogen absorption has

* Corresponding author.

E-mail address: n.kuganathan@imperial.ac.uk (N. Kuganathan).

been considered on the surface of Pd-decorated C₆₀ by El Mahdy [22]. Thus, C₆₀ provides different sites to capture species both internally (endohedral) and externally (exohedral).

This study uses density functional theory (DFT) together with dispersion corrections, to investigate the thermodynamical stability of gaseous volatile fission products (Kr, Xe, Br, I, Rb, Cs and Te) in order to understand whether they can be trapped by filters that incorporate C₆₀. For those species that may become bound to C₆₀, calculations have been performed to establish whether there is a preference for positions inside or on the surface of the fullerene cages and whether they become bound as atoms or in the form of dimers. DFT calculations, in addition to giving structural information, provide data on electronic properties, which are also discussed.

2. Computational methods

Calculations were carried out using the spin-polarized mode of DFT as implemented in the VASP [23,24] package. The exchange-correlation term was modelled using the generalized gradient approximation (GGA) parameterized by Perdew, Burke, and Ernzerhof (PBE) [25]. In all cases, we have used a plane-wave basis set with a cut-off value of 500 eV. Structural optimisations were performed using a conjugate gradient algorithm [26] and the forces on the atoms were obtained via the Hellman-Feynman theorem including Pulay corrections. In all optimized structures, forces on the atoms were smaller than 0.001 eV/Å and all the values in the atomic stress tensor were less than 0.002 GPa. All calculations were performed without using symmetry restrictions. All geometry optimisations were performed using a single *k*-point. To calculate the density of states (DOS), a 4 × 4 × 4 Monkhorst-Pack [27] *k* point mesh, which contains 36 *k* points was employed. A cubic super cell with a length of 25 Å was used for all configurations to ensure that adjacent structures do not interact (the largest linear dimension of a C₆₀ molecule was 7.10 Å). We define encapsulation energy (for single atom or dimer trapping inside the cage) and association energy (for single atom or dimer trapping outside the cage) by the following equation:

$$E_{\text{Enc/Assoc}} = E(\text{FP-C}_{60}) - E(\text{C}_{60}) - n E(\text{FP}) \quad (1)$$

where $E(\text{C}_{60})$ is the total energy for the isolated C₆₀ molecule, $E(\text{FP-C}_{60})$ is the total energy of the gaseous atom or atoms occupying the centre of the C₆₀ cage or interacting on the surface of C₆₀, $E(\text{FP})$ is the total energy of an isolated fission product (the reference state) and n is the number of fission product atoms considered in the process.

The inclusion of van der Waals (vdW) forces are particularly important for the interactions of the highly polarizable noble gases and transition metal atoms with C₆₀. Here, dispersion has been included by using the pair-wise force field as implemented by Grimme et al. [28] in the VASP package.

3. Results and discussion

3.1. Structural and electronic properties of C₆₀ fullerene molecule

A C₆₀ fullerene molecule is spherical with truncated icosahedral (*I_h*) symmetry. It consists of 12 pentagonal rings, 20 hexagonal rings and 32 faces as shown in Fig. 1a. There are two distinct alternate C–C and C=C bonds present in the molecule with the experimental bond lengths of 1.43 Å and 1.39 Å respectively [29]. In order to validate the computational parameters used in this study, we carried out an energy minimisation calculation to optimize the structure of a C₆₀ molecule. In the relaxed structure, we calculated

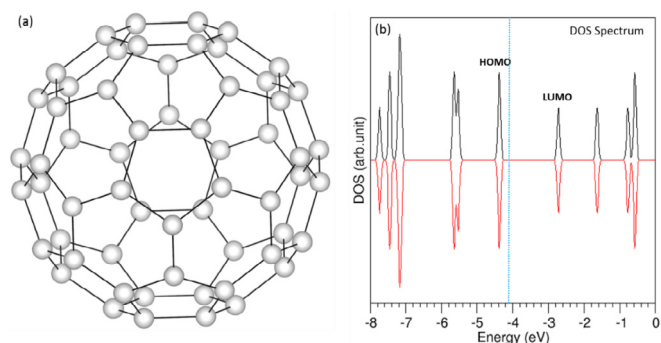


Fig. 1. (a) Optimised structure of a C₆₀ molecule and (b) its density of state spectra. The vertical dotted line, at ~ -4.10 eV, corresponds to the Fermi energy. (A colour version of this figure can be viewed online.)

the equilibrium bond distances, energy gap between the highest occupied molecular orbital (HOMO) and the lowest unoccupied molecular orbital (LUMO) and the net magnetic moment, to compare with experimental and other theoretical values.

The calculated bond lengths of C–C and C=C were 1.45 Å and 1.40 Å respectively, which agree well with experimental values [29] and other theoretical calculations [22]. The calculated HOMO–LUMO gap of the C₆₀ molecule is 1.55 eV, in good agreement with the value of 1.64 eV calculated by the DFT calculations of Goclon et al. [30]. Our calculation shows that the C₆₀ molecule is non-magnetic (see Fig. 1b) as predicted in previous studies [31].

3.2. Initial configurations

We considered six different sites for the absorption of fission products (FP). In the first configuration, the FP occupies the center of the cage [endohedral C₆₀ (**E**)], as shown in Fig. 2 (a). In terms of surface sites, there are five possible initial positions as shown in Fig. 2 (b) – (f). These are: (b) on top of the center hexagonal ring (**H**), (c) on top of the center pentagonal ring (**P**), (d) on top of a C–C bond between two hexagonal rings (**66**), (e) on top of a C–C bond between an hexagonal ring and a pentagonal ring (**65**) and (f) on top of a C atom on the C₆₀ cage (**C**).

3.3. Formation of single gaseous fission products interacting with C₆₀

First we consider the stability of the fission products (Xe, Kr, Br, I, Cs, Rb and Te) as single atoms occupying the centre of the C₆₀ cage. In relaxed configurations, the positions of the fission product atoms remain very close to the centre of the cage. The encapsulation energy for the fission products within the C₆₀ cage depends on the relative ionization potentials and electron affinities of the atom and the C₆₀ molecule but also the size of the atom or ion relative to the size of the internal volume of C₆₀. Fig. 3 (a) shows the calculated ionization potentials and the electron affinities of the fission product atoms and C₆₀ together with values reported in the data book [32]. Though the trend agrees well with the values reported in the data book, the current DFT calculations underestimate the first ionization potentials and overestimate the electron affinities. This is because of the ionization energies and electron affinities calculated from DFT orbital energies are usually poorer than those of Koopmans' theorem, depending on the exchange-correlation approximation employed [33,34].

Both Rb and Cs have lower ionization potentials and lower electron affinities than the C₆₀ molecule. A lower ionization potential enables the (easy) removal of the outermost electron from

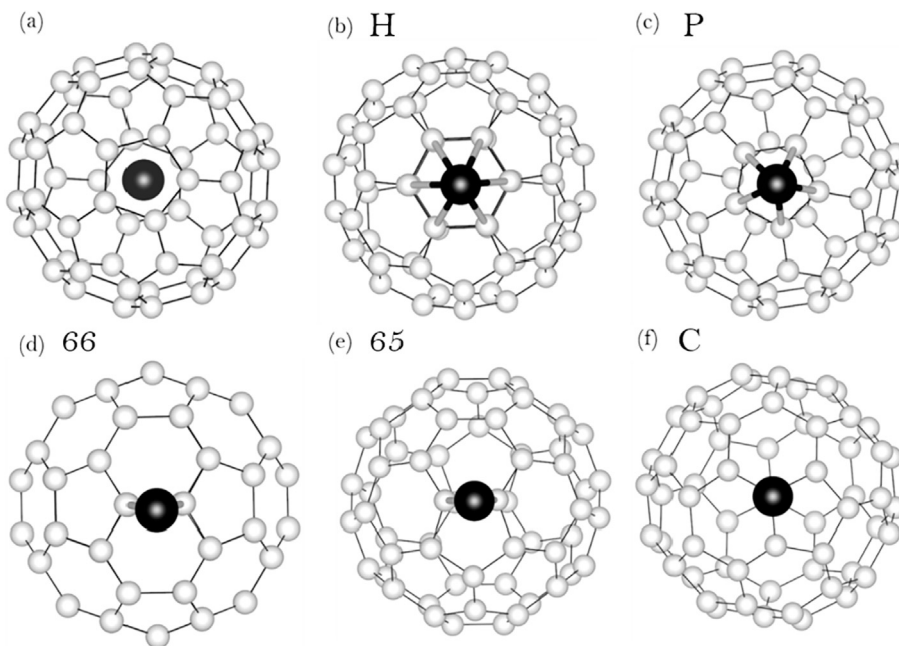


Fig. 2. Initial configurations considered for the FP: (a) absorbed in C_{60} endohedrally, (b) exohedrally adjacent to a six membered ring, (c) a five membered ring, (d) a C-C bond between two hexagons, (e) a C-C bond between an hexagon and a pentagon and (f) a C on the fullerene cage.

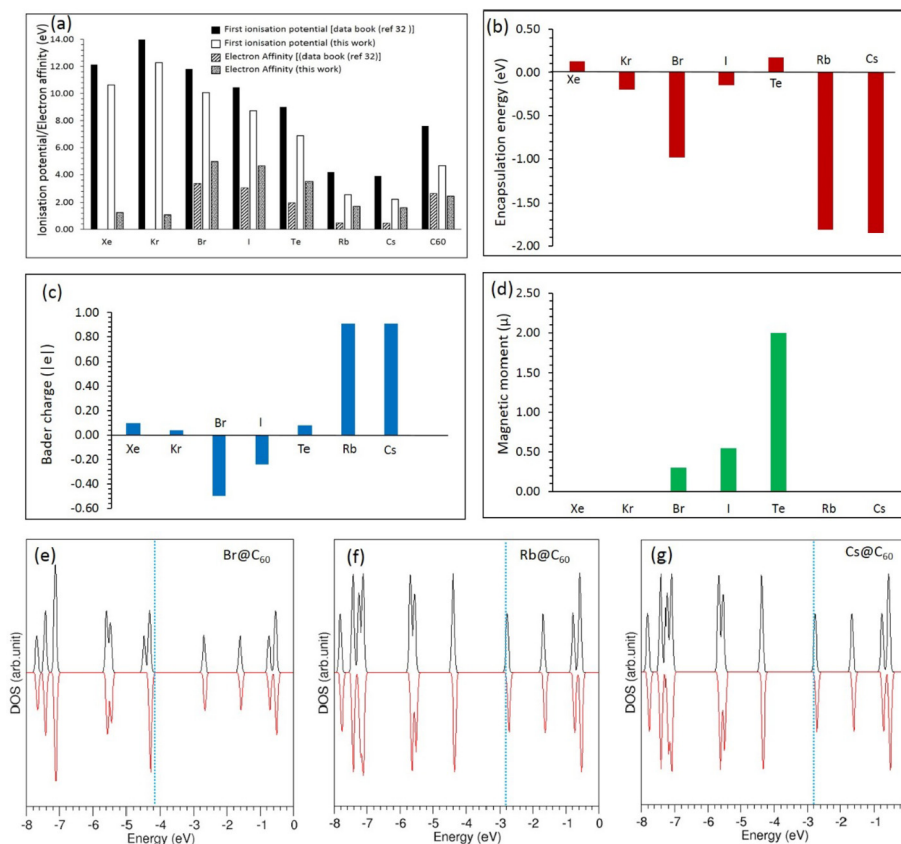


Fig. 3. (a) Calculated ionisation potential and electron affinity of volatile fission product atoms and C_{60} together with the values reported in the data book [32], (b) encapsulation energies, (c) Bader charge on atoms, (d) magnetic moment of the supercell and (e), (f) and (g) the total DOS of Br, Rb and Cs encapsulated in C_{60} respectively. (A colour version of this figure can be viewed online.)

Rb and Cs which is gained by the C_{60} molecule as it has a higher electron affinity. The calculations show that the encapsulation energies of Rb and Cs are highly exothermic [see Fig. 3b] meaning that they are more stable in the inner cage of C_{60} than as isolated atoms. Bader analysis also shows that both Rb and Cs gain a charge close to +1 by donating their outer s-electron to the C_{60} cage. Cs and Rb are therefore ions, which exhibit smaller radii than their corresponding atoms. The resultant complex can be considered as a donor-acceptor endohedral complex (M^+-C_{60}). Wang et al. [7] have calculated the formation energies for the endohedral encapsulation of Rb and Cs using Hartree-Fock calculations together with the Born-Haber cycle. In their calculations, they assumed that both metals lose one electron to form a +1 charge and C_{60} gains that lost electron to form -1 charge. The calculated formation energies by Wang et al. [7] for Rb and Cs are -1.91 eV and -1.64 eV respectively, in good agreement with our corresponding calculated values of -1.82 eV and -1.86 eV though the trend is slightly reversed.

Figs. 1 and 3d report that the magnetic moment of C_{60} is zero before and after the incorporation of Rb and Cs, indicating that encapsulation does not affect the magnetism. Calculations indicate that C_{60} exhibits zero magnetic moment. As Rb^+ and Cs^+ exhibit zero magnetic moment, overall complexes Rb^+-C_{60} and Cs^+-C_{60} are thus also non-magnetic. The total DOS for the Rb and Cs encapsulated in C_{60} are shown in Fig. 3f and (g) respectively. The encapsulation of Rb and Cs shift their DOS towards higher energies and the lowest unoccupied band of C_{60} becomes occupied by the s^1 electron transferred to C_{60} .

Turning now to the inert gasses, the outer electronic configurations of Xe and Kr are unaffected by encapsulation. This is a consequence of their higher ionization potentials. This is further supported by the very low encapsulation energies and the Bader charge. The encapsulation energies are a balance between attractive van der Waals forces of the polarisable atoms and Pauli repulsion of the electron clouds. Since Xe is large the Pauli repulsion is greater than exhibited by Kr and so Xe exhibits a slightly positive (unfavourable) encapsulation energy whereas for Kr the energy is slightly favourable.

The electron affinities of Br and I are reflected in the encapsulation energies and the Bader charges shown in Fig. 3; the encapsulation energy of Br is much more favourable than that of I due to the high electron affinity of Br but also because the smaller Br fits better inside C_{60} . The Bader charges on Br and I are -0.50 and -0.21 respectively. The outer electronic configuration of both Br and I are $s^2 p^5$ with one unpaired electron. As C_{60} and C_{60}^+ are non-magnetic and both Br and I gain electronic charge from C_{60} , the overall magnetic moment is reduced. The magnitude of the magnetic moment is reflected in the degree of the Bader charge. The total DOS (see Fig. 3e) shows that incorporation of Br introduces additional bands in the HOMO of C_{60} but the band gap is not much affected.

The positive encapsulation energy for Te reveals that it is unstable inside the cage due to its larger size and its inability to donate charge to C-C 66 single bonds. A small Bader charge and magnetic moment show that its outer electronic configuration is not altered.

Next, we consider how fission products can be trapped (or not) by the outer surface of C_{60} (i.e. the association energy). The behaviour of fission products occupying positions on the inner and outer faces of the C_{60} cage are different as the faces are convex and concave respectively. As explained earlier, we consider five possible initial exohedral configurations. These have been relaxed to give the final configurations and association energies. The relative association energies of each atom, reported in Table 1, are energies relative to the most stable site (which therefore has zero relative energy but not zero absolute association energy (see Fig. 4)).

The most stable exohedral position for Xe and Kr is on top of the

hexagonal ring (H). However, differences in energy compared with the other sites are very small, a consequence of how unreactive are the noble fission product gas atoms. The shortest FP-C distance, formation energies, Bader charge, magnetic moment of the supercell and the total DOS for the most stable configurations (identified in Table 1) are plotted in Fig. 4. While the (absolute) association energy is very small, it is negative due to the vdW interaction (see Fig. 4 a). Both a zero Bader charge and magnetic moment validate this conclusion. This is why the two noble gas atoms are almost 4.00 Å away from the surface of C_{60} . Interestingly the exohedral association energy for Kr is smaller than the encapsulation energy because Kr only interacts on the surface with six C atoms while inside C_{60} it interacts with the whole molecule. For Xe the situation is reversed: larger Xe is stable on the surface while its encapsulation energy is positive due to the large Pauli repulsion (compare values in Figs. 3 and 4).

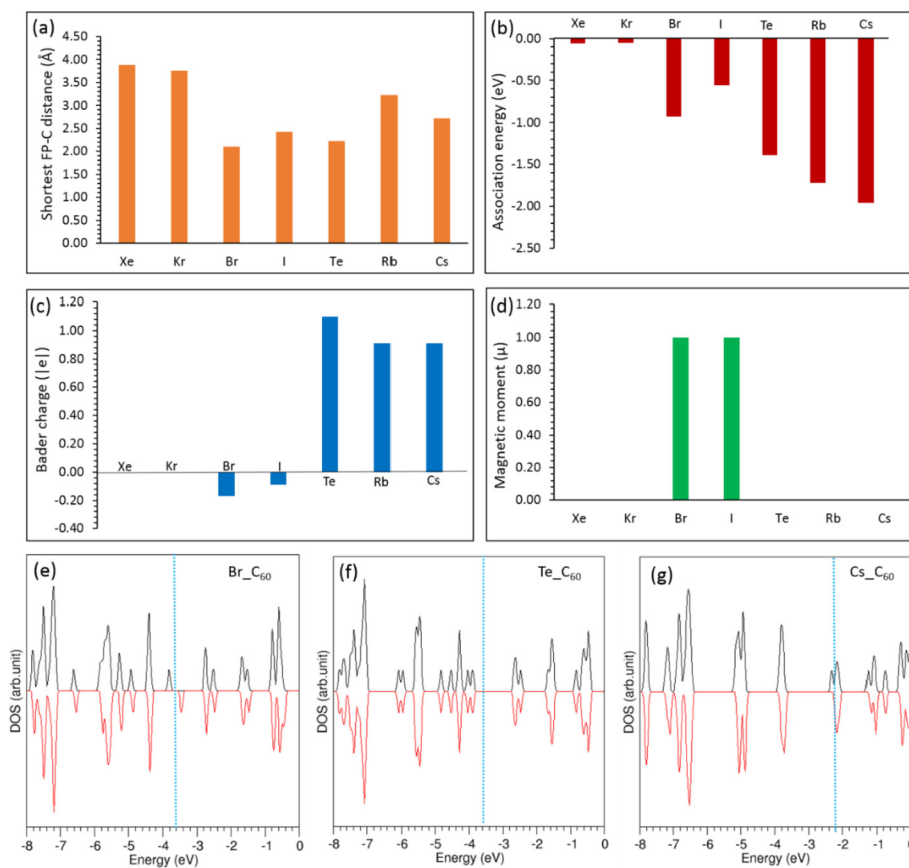
Br and I show a preference to be on top of the C-C bond, site (66), and gain a small charge (see Fig. 4c). That their magnetic moments are closer to 1 and Bader charge small means that their $s^2 p^5$ configuration with one spin up electron is unaltered. The formation energy for Br is -0.93 eV, a more favourable value than that for I (-0.56 eV). The association energy calculated for I by Kobayashi et al. [35] is -0.10 eV (without dispersion correction). This deviates from our calculated value of -0.56 eV where a dispersion correction is included. The stronger absorption of Br is due to its higher electron affinity compared to I and the shorter bond distance (C-Br v's C-I). Compared to Br and I inside C_{60} , less charge is transferred. This can be due to the halide atoms inside the cage being adjacent to and thus able to gain electron density from all the C atoms of C_{60} . However, inside the cage the bonding process is in opposition to Pauli repulsion; this is enough that I is more stable outside C_{60} . Conversely exohedral absorption of smaller Br is less favourable than inside the cage. Furthermore, with Br the Fermi level is shifted slightly to higher energies and the DOS spectrum of C_{60} is now dispersed with additional peaks. This is due to the chemical interaction of Br with the C atoms.

The (66) position is the preferred site for the Te, which loses ~1 electron (see Bader charge in Fig. 4 c) due to its lower electron affinity than C_{60} . Its formation energy is -1.39 eV showing strong absorption by the C_{60} surface, in contrast to endohedral adsorption. There is a significant bonding interaction between Te and carbon in the (66) position. This geometry of Te associated with (66) carbon can be described as an icosahedral triangle with the C-Te bond distance of 2.24 Å and C-C bond distance of 1.51 Å. The observed C-C bond distance of 1.51 Å is 0.11 Å longer than the C-C distance predicted for the (66) positions in other parts of the relaxed C_{60} configuration. It is further evidence of the significant interaction with Te. The Bader charge approximation shows that Te has lost 1.11 |e| and the carbons in the (66) position have gained those electrons with the ratio of 0.66:0.51. As the carbon in (66) position are now four coordinated, the π - π interaction is reduced with the elongation in the C-C bond. However, Te is unstable inside the cage and shows no interaction with C_{60} as evidenced by the Bader charge and magnetic moment. This is due to the larger size of the Te and its inability to donate charge to C-C 66 single bonds (in the relaxed configuration, Te occupies the center of the C_{60} and the distance between the Te and C-C 66 bond is 3.55 Å).

Rb and Cs exhibit strong association energies, essentially to the same extent as they did for encapsulation. This is because the alkali atoms have low ionization potentials and electron affinities. Bader analysis shows that both Rb and Cs form ~+1 charge donating their single s electrons to C_{60} . The resultant supercells exhibit zero magnetic moment. Fig. 4g shows there is a substantial Fermi energy shift to the higher energy levels upon absorption of Cs due to electron transfer to the C_{60} cage. The calculated association energy

Table 1Initial and final configurations (see Fig. 2 for definitions) of volatile fission products absorbed on C₆₀ exohedrally. The most stable configurations are highlighted in **bold**.

Initial Configuration	Final configuration and relative association energy (eV)						
	Xe	Kr	Br	I	Te	Rb	Cs
H	H, 0.00	H, 0.00	H, +0.52	H, +0.30	H, +1.19	H, 0.00	H, +0.02
P	P, +0.07	P, +0.03	P, +0.58	P, +0.32	P, +1.42	P, +0.07	P, +0.10
(66)	66, +0.02	66, +0.03	66, +0.23	66, +0.06	66, 0.00	66, +0.03	66, 0.00
(65)	65, +0.05	65, +0.03	C, 0.00	65, +0.13	65, +0.62	65, +0.18	65, +0.20
C	C, +0.06	C, +0.04	C, 0.00	C, 0.00	66, 0.00	C, +0.20	C, +0.22

**Fig. 4.** (a) Shortest distance between a C atom in C₆₀ and the exohedral FP, (b) association energy, (c) Bader charge on FP, (d) magnetic moment of the supercell and (e), (f) and (g) the total DOS of the most stable configurations of Br-C₆₀, Te-C₆₀ and Cs-C₆₀ respectively. (A colour version of this figure can be viewed online.)

of Cs derived by Kobayashi et al. [35] is -1.85 eV including the dispersion correction (without the dispersion correction the values is -1.49 eV) which is in good agreement with our current DFT + D value of -1.96 eV, and shows the necessity of including dispersion. Association energies calculated for of Rb and Cs by Sankar De et al. [36] are -1.59 eV and -1.70 eV respectively slightly deviating from our corresponding values of -1.72 eV and -1.96 eV due to the dispersion correction not being included in their calculations.

The encapsulation and association energies reported in Figs. 3 and 4 are for single atoms from single gas phase reference states. While this is physically realistic for Xe and Kr. It is clearly not for the other fission products that will form more complex gas phase species or react to form solids in their particular waste streams. Nevertheless, the energies reported thus are important components in relevant thermodynamic cycles and we hope prove useful to other studies. So, for example, it is possible that the reactive fission products may form diatomic species that are encapsulated or associated. The associated energies are also important

components in future thermodynamic cycles. Thus, as a first step towards more complex cycles we next report encapsulation and association energies of homonuclear diatomic molecules. These will also enable us to determine if encapsulation or association of atoms or molecules is the more favourable.

3.4. Formation of homonuclear dimers

Calculations were performed to investigate the energetics associated with homonuclear dimers both inside and outside C₆₀, with respect to isolated atoms and with respect to isolated dimer molecules (i.e. isolated atoms and molecules as reference states but normalised per atom). Only the reactive fission products were considered (i.e. those that form gas phase molecules). We considered Br, Rb and Cs for the formation of a dimer inside C₆₀ (see Fig. 5) whereas Br, I, Te, Rb and Cs dimers were considered as exohedral species (see Fig. 6).

The relaxed structures of dimers introduced inside the C₆₀ cage,

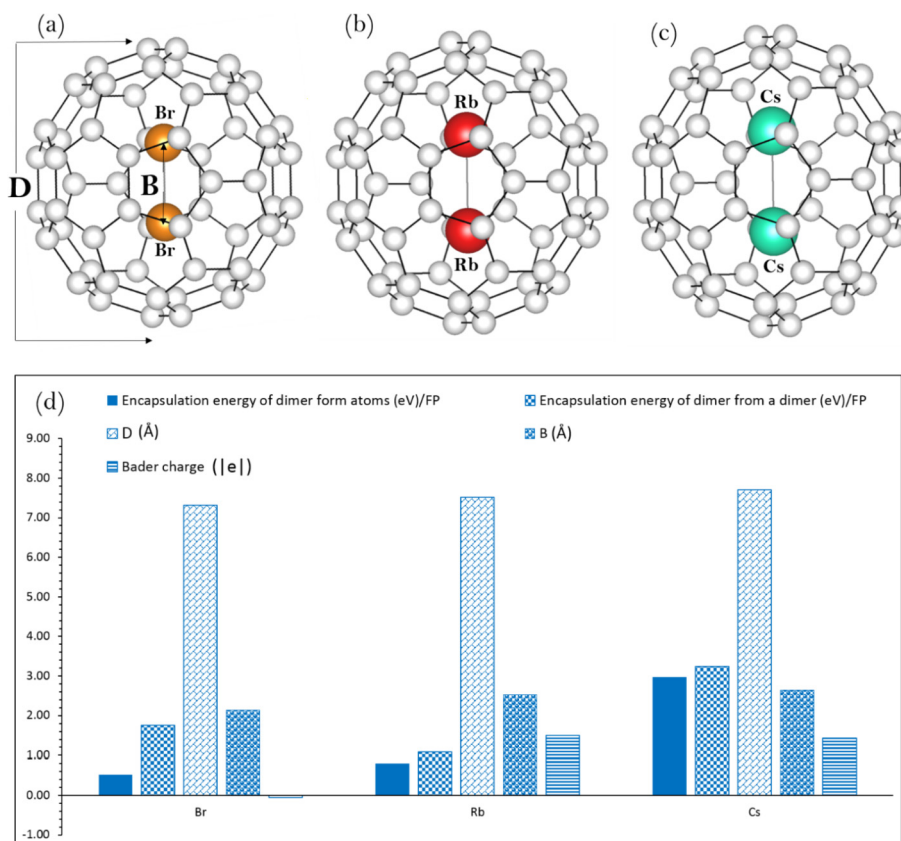


Fig. 5. Relaxed structures of (a) Br₂ (b) Rb₂ (c) Cs₂ encapsulated in C₆₀. (d) encapsulation energies from atoms, encapsulation energies of gas phase dimer (per atom), diameters of relaxed C₆₀ molecule, D, dimer bond lengths, B, and the Bader charge on dimers. (A colour version of this figure can be viewed online.)

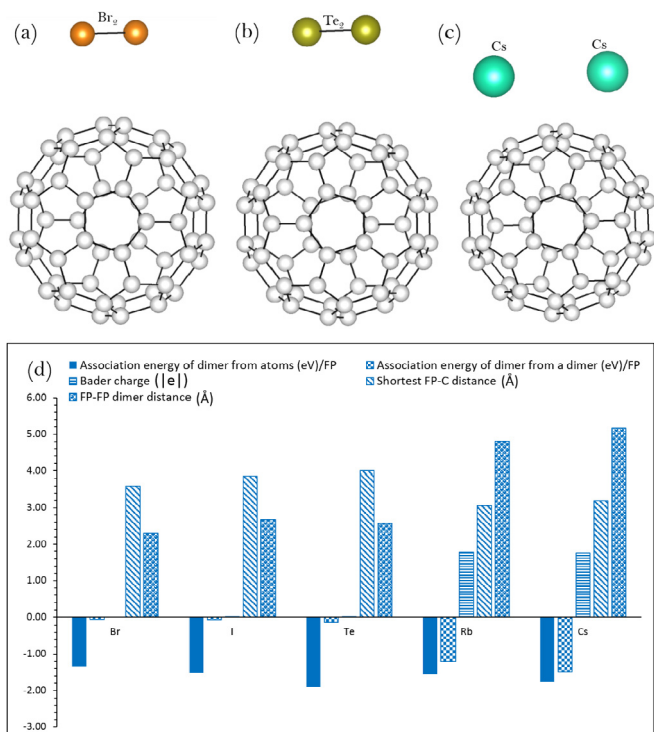


Fig. 6. Relaxed structures of (a) Br₂ (b) Te₂ (c) Cs₂ on the surface of C₆₀ and (d) association energies of FP dimers, shortest FP-C distances, FP-FP distances and the Bader charges on dimers. (A colour version of this figure can be viewed online.)

their encapsulation energies, and the diameter of the host C₆₀ molecules upon encapsulation, the dimer bond distances and the Bader charges on the dimers are shown in Fig. 5. Calculations show that all three dimers cause significant distortion of C₆₀; the degree of distortion is reflected in the large positive encapsulation energies and the diameters of the dimers containing C₆₀ (d) compared to dimer free C₆₀ (7.10 Å) (see Fig. 5d). The encapsulation energies for Br, Rb and Cs are positive meaning that they are not stable with respect to gas phase atoms or molecules. Endohedral encapsulation will therefore not be observed.

A dimer configuration for each species was allowed to adsorb on the surface of C₆₀. Fig. 6 shows: the relaxed structures of Br₂, Te₂ and Cs₂ and reports association energies (both from isolated atoms and isolated dimer reference states), the Bader charges on the dimers, shortest FP-C distance and the dimer bond length (D). The relaxed structures for I₂ and Rb₂ are similar to Br₂ and Cs₂ respectively.

Rb and Cs exhibit slightly smaller association energies per atom if adsorbed as a dimer to C₆₀ (Fig. 6) compared to single atoms (Fig. 4). Further, the separations of Rb-Rb (4.81 Å) and Cs-Cs (5.10 Å) (see Fig. 6d), are longer than in the corresponding gas phase diatomic molecules (4.30 Å for Rb₂ and 4.83 Å for Cs₂) consistent with these alkali metal species being non-bonded. This is because Rb and Cs interact strongly with C₆₀ with each atom donating ~1 electron (so that the Bader charge, reported in Fig. 6 is much greater than 1). The association energies per atom for Rb and Cs pairs are -1.20 eV and -1.48 eV respectively, less favourable than the values calculated for the corresponding single atoms, -1.72 eV and -1.95 eV respectively. Thus, while there is a driving force for a second alkali metal to join an alkali metal

exohedrally (i.e. -0.68 eV for the second Rb and -1.01 eV for the second Cs) if there are other unoccupied C_{60} molecules available, the second alkali metal will become associated with an unoccupied C_{60} molecule.

Br, I and Te all form covalently bonded dimer molecules with bond lengths values when exohedrally absorbed (Fig. 6), that are very similar to data from experimental (Br_2 2.28 Å, I_2 2.66 Å and Te_2 2.56 Å) [37] and calculated (Br_2 2.31 Å, I_2 2.68 Å and Te_2 2.58 Å) gas phase species. This indicates these molecules are not bonded to C_{60} . The long FP-C distances are further evidence of this (see Fig. 6). While there are strong association energies for Br_2 , I_2 and Te_2 per atom, from the reference states of atoms, for the dimers to associate, the association energies per dimer from an existing dimer are small (i.e. from the dimer reference state). The dimer association is a result of the induced-induced polarization observed on each of the atoms of the dimer, though the overall Bader charge is zero, consistent with a non-bonded interaction. The rationale for this is that a single atom has considerable electronegativity based on gaining charge that will occupy a p -orbital, whereas additional negative charge to a dimer has to occupy a higher energy σ^* molecular orbital. Thus, while Br, I and Te demonstrate a preference to form exohedral dimers rather than forming two single atoms on the surfaces of two different C_{60} molecules, that driving force is a consequence of the covalent bond between the two fission product species. Thus, the association of these dimers is quite different to that of their atoms, in contrast to the situation for the alkali metals.

Table 2 reports the energetics for taking homonuclear diatomic gas phase molecules and associating them with C_{60} either as atoms or molecules, assuming an abundance of C_{60} molecules. These values show that Rb_2 and Cs_2 dissociate and associate as single positive ions. Conversely, Br_2 , I_2 and Te_2 stay as strong covalently bonded molecules, weakly associating via vdW interactions.

3.5. Heteronuclear dimer association and endohedral/exohedral pairs

Finally, we have considered interactions from heteronuclear diatomic molecule reference states. Consider first CsBr: there are two different fission atoms (Cs and Br) interacting with C_{60} in four different ways. The four configurations for Cs and Br are: Fig. 7 (a) with Br encapsulated by C_{60} while Cs is associated exohedrally, Fig. 7b where Cs is encapsulated by C_{60} and Br associated exohedrally, Fig. 7c where both Cs and Br are associated as single atoms exohedrally and Fig. 7 (d) Cs and Br are associated exohedrally as a pair. This enables an investigation of whether Cs encapsulation facilitates Br association or vice versa. We have also considered Cs and I as a pair but only associating with C_{60} exohedrally since neither Cs nor I show any preference for endohedral encapsulation.

The energies to encapsulate and associate CsBr and CsI are reported in Table 3. Total energies for configurations (geometries) as in Fig. 7d are always more favourable than those as in Fig. 7c. Thus, exohedral molecule energies discussed will be with respect only to Fig. 7d. The values with respect to single atoms can be used to first assess how much more strongly a Cs, Br or I atom will become

trapped if an opposite heteronuclear species is already present (note: energies with respect to single gas atom reference states). For example, Table 3 reports Br is encapsulated to C_{60} with an energy of -0.98 eV but if Cs is already present as an exohedral species the Br encapsulation energy increases to -2.29 eV. Similarly for the Cs exohedral association energy raises from -1.96 eV to -3.28 eV if Br is already present as an endohedral species. Equivalent combinations show similar gains in energy. Table 3 also shows that Bader charges on Br and Cs increase when both species are present. The same effect is reported for Cs and I.

Table 3 also reports energies to trap CsBr and CsI molecules. For CsBr both Br endohedrally and exohedrally are considered with Cs considered exohedrally. In both cases CsBr is trapped but not strongly and there is a preference for both species being exohedral. The energy for Cs encapsulated and Br associated exohedrally is also reported in Table 3. In this case the energy positive (i.e. unfavourable) reflecting the strong preference for Cs to be an exohedral species rather than endohedral. The association energy of CsI (both exohedral species) is similar to that of CsBr and small consistent with these molecules being trapped by vdW forces. The net Bader charge on the CsBr and CsI molecules exohedral to C_{60} is almost zero, again consistent with a non-bonded interaction. The energies are similar to those observed for homonuclear dimers (Br_2 , I_2 and Te_2). For CsI, the adsorption energy with respect to the dimer derived by Kobayashi et al. [35] is -0.12 eV without dispersion and -0.62 eV with dispersion (though we assume only for Cs). The current calculation shows that the association of CsI is -0.42 eV though we include dispersion for Cs and I thus importantly between Cs and I.

Finally, we calculate the energy difference (reaction) between $\frac{1}{2}$ Br_2 (and $\frac{1}{2}$ I_2) exohedrally trapped and Cs (and Rb) trapped as ions to form CsBr (and CsI) trapped exohedrally. In both cases the heteronuclear molecules are more stable; by -1.24 eV for CsBr and -0.98 eV CsI.

4. Conclusions

C_{60} is a candidate active material for filters used in nuclear plants where volatile fission products must be separated from effluent gases. In this context it has good mechanical and chemical properties. Using density functional theory together with a dispersion correction and vdW forces, we have investigated the capacity of C_{60} to trap key volatile fission products.

Consider first trapping of atoms from the reference state of atoms. Xe and Kr are weakly trapped via vdW forces with exohedral association energies of about -0.05 eV. Kr is endohedrally trapped with a stronger encapsulation energy of -0.20 eV but Xe, being much larger, is not trapped endohedrally. Single gaseous Rb and Cs atoms exhibit endohedral encapsulation energies of -1.82 eV and -1.86 eV respectively (i.e. strongly exothermic). The outer surface of the C_{60} also exothermically absorbs Rb and Cs as single gaseous atoms with similar energies of -1.72 eV for Rb and -1.96 eV for Cs. Thus endohedral and exohedral behaviour is similar. Calculated trapping energies for Br, I and Te as single atom

Table 2
Exohedral association energies of FP atoms and homonuclear diatomic molecules from molecule reference states.

	Most stable position for atoms/dimers associating with C_{60} exohedrally				
	Rb	Cs	Br	I	Te
Most stable site	H	(66)	C	C	(66)
Association energy of an atom (eV/atom) with respect to dimer	-1.44	-1.70	$+0.34$	$+0.56$	$+0.38$
	Rb_2	Cs_2	Br_2	I_2	Te_2
Association energy of dimer (eV/atom) with respect to dimer	-1.20	-1.48	-0.06	-0.07	-0.13

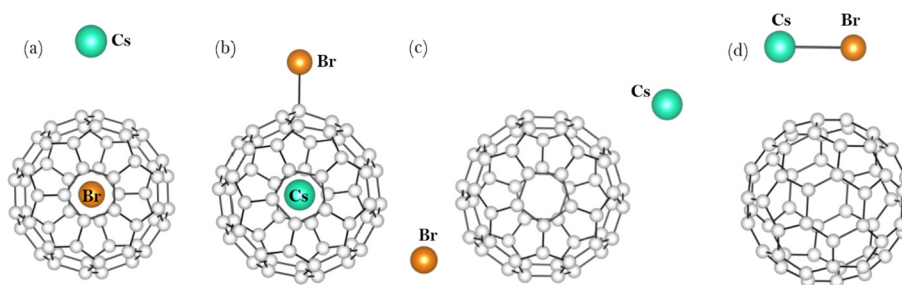


Fig. 7. Relaxed configurations of (a) endohedral Br with exohedral Cs, (b) endohedral Cs with exohedral Br and (c) exohedral Cs with exohedral Br as single atoms and (d) exohedral Cs with exohedral Br as a pair. (A colour version of this figure can be viewed online.)

Table 3
Encapsulation or association energies and Bader charge calculated for the fission atoms interacting C_{60} .

Reaction	Encapsulation/Association energy (eV/atom) with respect to atoms	Bader charge [e]	
		Br or I	Cs
$Br + C_{60} \rightarrow Br_{endo}C_{60}$	-0.98	-0.50	-
$Br + Cs_{exo}C_{60} \rightarrow Br_{endo}Cs_{exo}C_{60}$	-2.29	-0.71	+0.94
$Cs + C_{60} \rightarrow Cs_{exo}C_{60}$	-1.96	-	+0.91
$Cs + Br_{endo}C_{60} \rightarrow Cs_{exo}Br_{endo}C_{60}$	-3.28	-0.71	+0.94
$Br + C_{60} \rightarrow Br_{exo}C_{60}$	-0.93	-0.17	-
$Br + Cs_{exo}C_{60} \rightarrow Br_{exo}Cs_{exo}C_{60}$	-1.31	-0.37	+0.94
$Br + Cs_{endo}C_{60} \rightarrow Br_{exo}Cs_{endo}C_{60}$	-1.59	-0.26	+0.91
$Cs + C_{60} \rightarrow Cs_{endo}C_{60}$	-1.85	-	+0.91
$Cs + Br_{exo}C_{60} \rightarrow Cs_{endo}Br_{exo}C_{60}$	-2.50	-0.26	+0.91
$Cs + Br_{exo}C_{60} \rightarrow Cs_{exo}Br_{exo}C_{60}$	-2.34	-0.37	+0.94
$I + C_{60} \rightarrow I_{exo}C_{60}$	-0.56	-0.09	-
$I + Cs_{exo}C_{60} \rightarrow I_{exo}Cs_{exo}C_{60}$	-1.03	-0.37	+0.94
$Cs + I_{exo}C_{60} \rightarrow Cs_{exo}I_{exo}C_{60}$	-2.43	-0.37	+0.94
	with respect to dimer (eV/atom)		
$CsBr + C_{60} \rightarrow Cs_{exo}Br_{endo}C_{60}$	-0.07	-0.71	+0.94
$CsBr + C_{60} \rightarrow Cs_{endo}Br_{exo}C_{60}$	+0.34	-0.26	+0.91
$CsBr + C_{60} \rightarrow (Cs_{exo}Br_{exo})C_{60}$	-0.17	-0.77	+0.86
$CsI + C_{60} \rightarrow (Cs_{exo}I_{exo})C_{60}$	-0.21	-0.71	+0.85

species from the gas phase showed different behaviours. Br is exohedrally and endohedrally trapped with energies of -0.93 eV and -0.98 eV respectively. I exhibits an encapsulation energy of -0.2 eV but an association energy of -0.6 eV. For Te the difference is even greater with an endothermic encapsulation energy and an exothermic association energy of -1.4 eV.

A dimer will not form inside the cage of C_{60} for any species because there is insufficient volume, as evidenced by the distortion introduced by the dimer (see Fig. 5). However, the outer surface has the ability to trap Br_2 , I_2 or Te_2 dimers *via* non-bonding van-der Waals interactions with association energies per atom of only around -0.1 eV per atom. Conversely, Rb_2 and Cs_2 are strongly absorbed but as single atoms, forming positive charged ions as these ions are highly stable.

Finally, trapping of $CsBr$ and CsI molecules was considered. Both showed a preference to be endohedral molecules with encapsulation energies of just under -0.2 eV per atom.

Acknowledgements

We thank the EPSRC for funding as part of the “PACIFIC” programme (grant code EP/L018616/1). Computational facilities and support were provided by High Performance Computing Centre at Imperial College London. Mr. Conor O. T. Galvin is acknowledged for helpful discussions.

References

[1] V.M. Erfmrenkov, Radioactive waste management at nuclear plants, IAEA Bull. 4 (1989) 37–42.

[2] M.I. Ojovan, W.E. Lee, An Introduction to Nuclear Waste Immobilisation, second ed., Elsevier, Oxford, U.K, 2014.

[3] A. Karhu, Methods to Prevent the Source Term of Methyl Iodide during a Core Melt Accident (NKS-13) Denmark, 1999.

[4] D.F. Sava, M.A. Rodriguez, K.W. Chapman, P.J. Chupas, J.A. Greathouse, P.S. Crozier, T.M. Nenoff, Capture of volatile iodine, a gaseous fission product, by zeolitic imidazolate Framework-8, J. Am. Chem. Soc. 133 (2011) 12398–12401.

[5] M.S. Dresselhaus, G. Dresselhaus, P.C. Eklund, Science of Fullerenes and Carbon Nanotubes, Academic Press, San Diego, 1996.

[6] H.W. Kroto, A.W. Allaf, S.P. Balm, C_{60} : buckminsterfullerene, Chem. Rev. 91 (1991) 1213–1235.

[7] Y. Wang, D. Tománek, R.S. Ruoff, Stability of $M@C_{60}$ endohedral complexes, Chem. Phys. Lett. 208 (1993) 79–85.

[8] E. Broclawik, A. Eilmes, Density functional study of endohedral complexes $M@C_{60}$ ($M=Li, Na, K, Be, Mg, Ca, La, B, Al$): electronic properties, ionization potentials, and electron affinities, J. Chem. Phys. 108 (1998) 3498–3503.

[9] K. Kikuchi, K. Kobayashi, K. Sueki, S. Suzuki, H. Nakahara, Y. Achiba, K. Tomura, M. Katada, Encapsulation of radioactive ^{159}Gd and ^{161}Tb atoms in fullerene cages, J. Am. Chem. Soc. 116 (1994) 9775–9776.

[10] S.K. Saha, D.P. Chowdhury, S.K. Das, R. Guin, Encapsulation of radioactive isotopes into C_{60} fullerene cage by recoil implantation technique, Nucl. Instrum. Methods Phys. Res. Sect. B Beam Interact. Mater. Atoms 243 (2006) 277–281.

[11] A.K. Srivastava, S.K. Pandey, N. Misra, Encapsulation of lawrencium into C_{60} fullerene: $Lr@C_{60}$ versus $Li@C_{60}$, Mater. Chem. Phys. 177 (2016) 437–441.

[12] J. Lu, Y. Zhou, X. Zhang, X. Zhao, Structural and electronic properties of endohedral phosphorus fullerene $P@C_{60}$: an off-centre Displacement of P inside the cage, Mol. Phys. 99 (2001) 1199–1202.

[13] S.C. Cho, T. Kaneko, H. Ishida, R. Hatakeyama, Nitrogen-atom endohedral fullerene synthesis with high efficiency by controlling plasma-ion irradiation energy and C_{60} internal energy, J. Appl. Phys. 117 (2015), 123301.

[14] T. Braun, H. Rausch, Endohedral incorporation of argon atoms into C_{60} by neutron irradiation, Chem. Phys. Lett. 237 (1995) 1995.

[15] Z.Y. Wang, K.H. Su, H.Q. Fan, Y.L. Li, Z.Y. Wen, Mechanical, Electronic properties of endofullerene $Ne@C_{60}$ studied via structure distortions, Mol. Phys. 106 (2008) 703–716.

[16] P.F. Weck, E. Kim, K.R. Czerwinski, D. Tománek, Structural and magnetic

- properties of $T_{C_n}@C_{60}$ endohedral metallofullerenes: first-principles predictions, *Phys. Rev. B* 81 (2010), 125448.
- [17] H. Minezaki, K. Oshima, T. Uchida, T. Mizuki, R. Racz, M. Muramatsu, T. Asaji, A. Kitagawa, Y. Kato, S. Biri, Y. Yoshida, Synthesis of Fe- C_{60} complex by ion irradiation, *Nucl. Instrum. Methods Phys. Res. Sect. B Beam Interact. Mater. Atoms* 310 (2013) 18–22.
- [18] J.R. Heath, S.C. O'Brien, Q. Zhang, Y. Liu, R.F. Curl, F.K. Tittel, R.E. Smalley, *J. Am. Chem. Soc.* 107 (1985) 7779–7780.
- [19] N. Kuganathan, J.C. Green, H.-J. Himmel, *N. J. Chem.* 30 (2006) 1253–1262.
- [20] Q. Sun, Q. Wang, P. Jena, Y. Kawazoe, Clustering of Ti on a C_{60} surface and its effect on hydrogen storage, *J. Am. Chem. Soc.* 127 (2005) 14582–14583.
- [21] B. Özdamar, M. Boero, C. Massobrio, D. Felder-Flesch, S.L. Roux, Systems as tunable- gap building blocks for nanoarchitecture and nanocatalysis, *J. Chem. Phys.* 143 (2015) 114308.
- [22] A.M.E. Mahdy, Dft study of hydrogen storage in Pd-Decorated C_{60} fullerene, *Mol. Phys.* 113 (2015) 3531–3544.
- [23] G. Kresse, J. Furthmüller, Efficient iterative schemes for ab initio total-energy calculations using a plane-wave basis set, *Phys. Rev. B* 54 (1996) 11169–11186.
- [24] G. Kresse, D. Joubert, From ultrasoft pseudopotentials to the projector augmented-wave method, *Phys. Rev. B* 59 (1999) 1758–1775.
- [25] J.P. Perdew, K. Burke, M. Ernzerhof, Generalized gradient approximation made simple, *Phys. Rev. Lett.* 77 (1996) 3865–3868.
- [26] W.H. Press, B.P. Flannery, S.A. Teukolsky, W.T. Vetterling, *Numerical Recipes. The Art of Scientific Computing*, Cambridge Univ. Press, Cambridge, 1986, 818 pp.
- [27] H.J. Monkhorst, J.D. Pack, Special points for brillouin-zone integrations, *Phys. Rev. B* 13 (1976) 5188–5192.
- [28] S. Grimme, J. Antony, S. Ehrlich, H. Krieg, A consistent and accurate ab initio parametrization of density functional dispersion correction (Dft-D) for the 94 elements H-Pu, *J. Chem. Phys.* 132 (2010), 154104.
- [29] J.M. Hawkins, *Accounts Chem. Res.* 25 (1992) 150–156.
- [30] J. Goclon, K. Winkler, J.T. Margraf, Theoretical investigation of interactions between palladium and fullerene in polymer, *RSC Adv.* 7 (2017) 2202–2210.
- [31] N.M. Umran, R. Kumar, Theoretical investigation of endohedral complexes of Si and Ge with C_{60} molecule, *Phys. B Condens. Matter* 437 (2014) 47–52.
- [32] D.R. Lide, *CRC Handbook of Chemistry and Physics*, 86th ed., CRC, Boca Raton, FL, 2005.
- [33] P. Politzer, F. Abu-Awwad, A comparative analysis of Hartree-Fock and Kohn-Sham orbital energies, *Theo. Chem. Acc.* 99 (2) (1998) 83–87.
- [34] S. Hamel, P. Duffy, M.E. Casida, D.R. Salahub, Kohn-Sham orbitals and orbital energies: fictitious constructs but good approximations all the same, *J. Electron. Spectrosc. Relat. Phenom.* 123 (2002) 345.
- [35] T. Kobayashi, K. Yokoyama, Theoretical study of the adsorption of Cs, Cs^+ , I, I^- , and CsI on C_{60} fullerene, *J. Nucl. Sci. Technol.* 53 (2016) 1489–1493.
- [36] D. Sankar De, J.A. Flores-Livas, S. Saha, L. Genovese, S. Goedecker, Stable structures of exohedrally decorated C_{60} -fullerenes, *Carbon* 129 (2018) 847–853.
- [37] K.P. Huber, G. Herzberg, *Molecular Spectra and Molecular Structure— IV. Constants of Diatomic Molecules*, Van Nostrand Reinhold, New York, 1979.